Available online at www.sciencedirect.com
ScienceDirect
Polymer 48 (2007) 7145–7155
polymer
www.elsevier.com/locate/polymer

Structure and electric properties of poly(vinylidene fluoride–tetrafluoroethylene) copolymer studied with density functional theory

Zhi-Yin Wang [a,c], Ke-He Su [b,*], Hui-Qing Fan [a], Zhen-Yi Wen [d]

[a] *State Key Laboratory of Solidification Processing, School of Materials Science and Engineering, Northwestern Polytechnical University, Xi'an, Shaanxi 710072, PR China*
[b] *School of Natural and Applied Sciences, Northwestern Polytechnical University, Xi'an, Shaanxi 710072, PR China*
[c] *School of Chemistry and Environmental Sciences, Shaanxi University of Technology, Hanzhong, Shaanxi 723000, PR China*
[d] *Institute of Modern Physics, Northwest University, Xi'an, Shaanxi 710068, PR China*

Received 26 April 2007; received in revised form 14 August 2007; accepted 12 September 2007
Available online 23 September 2007

Abstract

The internal rotation, geometry, energy, vibrational spectra, dipole moments and molecular mean polarizabilities of poly(vinylidene fluoride–tetrafluoroethylene) (P(VDF–TeFE)) of α- and β-chain models were studied with density functional theory at B3PW91/6-31G(d) level and compared with those of poly(vinylidene fluoride) homopolymer and P(VDF–TrFE) copolymer. The electric properties, chain conformation and stability of the copolymer influenced by the chain length and TeFE content were examined. Based on the internal rotation curves of P(VDF–TeFE) dimer models (H[CH_2CF_2–CF_2CF_2]H and H[CF_2CH_2–CF_2CF_2]H), the conformational angles, relative stabilities of α- and β-conformation, and the transition energy barriers of β → α and α → β were discussed. The results show that the β-conformation is more stable than the α-conformation thermodynamically and the β → α transition in P(VDF–TeFE) is more difficult than that in PVDF. Thus the copolymer should be in favor of preventing the piezoelectric phase from depolarization. The ideal β-chains are curved with a radius of about 30 Å, which is very close to those in both PVDF and P(VDF–TrFE). Similar to P(VDF–TrFE), the α-chain P(VDF–TeFE) containing 0.50 mole fraction of TeFE is also a *helical* structure. However, the α-chain with 0.33–0.20 mole fraction of TeFE are almost linear in structure, which might be responsible for enhancing crystallinity of the copolymer. The contribution of average dipole moment per monomer unit in the β-chain is affected by the chain curvature and TeFE content, and there is a weakly parabolic dependence on the VDF content. The chain length and TeFE content will not significantly affect the mean polarizability per monomer unit. The calculations show that there are some characteristic vibrational modes that may be used in the identification of the α- and β-phase P(VDF–TeFE) with different TeFE contents.

Keywords: Polymer physical chemistry; DFT; P(VDF–TeFE)

1. Introduction

Poly(vinylidene fluoride) (PVDF), the well-known ferroelectric polymer [1–4], is a material that is usually synthesized as a mixture of ordered and disordered phases. It is necessary that the polymer film should be post-processed into ferroelectric phase (or β-phase) before applications. The post-processing procedures are generally complex, for instance, subjecting the film to mechanical deformation [5,6], electron irradiation [7], uniaxial drawing [8] and crystallization under high pressure [9] or high electric field [10,11]. It is desirable to obtain a polymer with piezoelectric phase by simple treatment.

Extensive attention has been paid to the copolymers of vinylidene fluoride (VDF) with trifluoroethylene (TrFE) [12–16] and tetrafluoroethylene (TeFE) [14–16]. The copolymers were demonstrated to possess ferroelectricity over a wide range of composition [17,18]. The advantage of the copolymers is that it may crystallize directly from the melting state into a

* Corresponding author. Tel.: +86 29 88493915; fax: +86 29 88493325.
E-mail address: sukehe@nwpu.edu.cn (K.-H. Su).

0032-3861/$ - see front matter © 2007 Elsevier Ltd. All rights reserved.
doi:10.1016/j.polymer.2007.09.029

piezoelectric crystal phase, which eliminates the complicated post-processing procedures.

In previous papers of PVDF [19] and P(VDF–TrFE) [20], based on first principle density functional theory (DFT) calculations, we presented some explanations of structure–property relationships. Encouraged by the interesting results, we will extend the study to poly(vinylidene fluoride–tetrafluoroethylene) (P(VDF–TeFE)) copolymer system in this work. The structural and energetic implications with increasing TeFE content in P(VDF–TeFE) copolymers will be examined in order to achieve a better understanding of the system.

Compared with VDF, the TrFE monomer exhibits lower polarity and TeFE has no polarity. However, both P(VDF–TrFE) and P(VDF–TeFE) can be grown in higher crystallinity [21–25] resulting in stronger polarization and piezoelectric response than the semicrystalline PVDF. Among the known copolymers, P(VDF–TeFE) is also an important and one of the most widely used ferroelectric polymers [26,27]. The *trans* conformation in the copolymers may be stabilized with TeFE units and the crystallinity can be as high as 90% [28]. Such P(VDF–TeFE) copolymers were firstly examined in 1968 by Lando and Doll [29], showing that the copolymer containing at least 0.07 mole fraction of TeFE is able to crystallize into the *all-trans* conformation of the ferroelectric β-phase. Kochervinskij et al. have studied the piezoelectricity and structure of the monoaxial stretched β-P(VDF–TeFE) copolymer at different temperatures [30], the conditions of thermal treatment and the structure of the cold-stretched film [31,32]. X-ray, IR, Raman spectroscopies and other technological means have been employed to study the crystal structure, electrostatic poling, phase transition behavior and ferroelectric hysteresis loops [15,16,33–41]. The results show that in the sample with VDF–TeFE of 81/19 (mole ratio) the conformation change between the *trans* (low temperature) and *gauche* (high temperature) phases occurs in the temperature region close to the melting point with thermal hysteresis. The sample with VDF–TeFE of 75/25 (mole ratio) shows similar transition between low and high temperature phases but *via* an additional disordered cooled phase. The behavior is close to that observed in P(VDF–TrFE) copolymer with VDF–TrFE of 65/35 (mole ratio) [38]. In fact, P(VDF–TeFE) copolymers have been found widely to show ferroelectric phase transition similar to P(VDF–TrFE) samples [16,28,39–41].

In understanding the structure–property relation of P(VDF–TeFE) theoretically, Farmer, et al. [42] studied the structure and properties using potential energy calculations to determine the chain conformation and packing energies. Their work shows that the introduction of TeFE may cause the *all-trans* chains in a lower energy conformation. The greater proportion of bulky tetra-fluorine atoms in the copolymer will prevent the chains from accommodating α-chain (or $tgtg'$, where g refers *gauche* and t refers *trans*, and a prime in g' refers the dihedral angle being opposite to the g conformation with respect to the reference plane t) conformation. Therefore, copolymers are able to crystallize directly at room temperature into a ferroelectric β-phase [43,44] that possesses polar unit cells (similar to the β-phase of PVDF homopolymer). The copolymer can also be electro-processed into an enhanced piezoelectric material immediately after crystallization. Recently, Nakhmanson et al. [14] investigated the polar properties of the β-phase of PVDF and its copolymers with TrFE and TeFE using an *ab initio* multigrid-based total-energy method. Their calculations show that polarization in such polymers is described by cooperative, quantum-mechanical interactions between polymer chains, which cannot be viewed as a superposition of rigid dipoles. For β-PVDF, the monomer dipole moment is increased by 50% (from 2 to 3 Debye) if the isolated chains are brought together to form a crystal. In the copolymers, a weakly parabolic dependence of monomer dipole moments on concentration is obtained.

However, there are still a number of questions that remain unclear. For example, TeFE monomer does not inject new chemical unit into the copolymer chain since the $-CF_2-$ segment is already presented in PVDF. As Lando and Doll [29] pointed out, P(VDF–TeFE) copolymer can be viewed essentially as PVDF chains with an increased content of *head-to-head* but not *tail-to-tail* defects ($-CF_2-$ being viewed as the head). TrFE addition is subjected to tacticity defects and thus introduces a new variable (third chemical species $-CHF-$) to the copolymer chains, rendering them atactic. However, the structure of the paraelectric phase in P(VDF–TeFE) appears to be analogous to that of P(VDF–TrFE) [16]. Comparison of the structural features between these two types of copolymers will provide important information for understanding the structure and phase transition of fluorine copolymers. It will be interesting to understand how TeFE content will affect the conformation and energy of the copolymer and, specifically, what role TeFE variety would play in the polymorphism of P(VDF–TeFE). This work will thus explore the structure and energy implications in increasing TeFE in P(VDF–TeFE) copolymers with the first principle method as that in Ref. [20] and the results will be compared with P(VDF–TrFE). The similarities and distinctions in structural characteristics will be emphasized. Internal rotation potentials, geometries and electrical properties of $tgtg'$ and ttt (all-trans) chains P(VDF–TeFE) will be examined. For different conformations, energy differences, permanent dipole moment, mean polarizability per monomer and vibrational spectra will be analyzed. Some characteristic vibrational modes of α- and β-chain, which might be helpful in identification of the α- and β-phase copolymers, will be assigned and compared with the experiments.

2. Theoretical method

Density functional theory, owing to including the electronic correlations, is commonly believed to be the theoretical method that is able to describe the geometries and vibrational frequencies of molecules quite well [45] and can be used in larger molecular systems [45–53]. In fact, DFT has been widely used in polymer triumphantly [54–61]. Among a number of methods, B3PW91 has been examined to be the best in reproducing the equilibrium structures in our systematic comparison [62,63] of geometry optimizations. We therefore employed B3PW91 (a combination of the Becke's

three-parameter (B3) exchange functional [64,65] and the correlation functional of Pedew and Wang, PW91 [66]) in the present study. To compare the results with those of our previous work on PVDF [19] and P(VDF–TrFE) [20], the same basis set, 6-31G(d) (valence double ξ plus d polarization functions on heavy atoms), was chosen. The GAUSSIAN-03 package [67] was used to perform the calculations on internal rotation potentials of the dimer models, geometry optimizations and vibration analyses of the α- and β-chain P(VDF–TeFE)s with different chain lengths (denoted by n as follows) and TeFE contents as well as molecular energy and dipole moment vectors (μ_x, μ_y, μ_z). The models are H[(CH_2CF_2)–(CF_2CF_2)]$_m$H ($n = 2m$), H[$(CH_2CF_2)_2$–(CF_2CF_2)]$_m$H ($n = 3m$), H[$(CH_2CF_2)_3$–(CF_2CF_2)]$_m$H ($n = 4m$), H[$(CH_2CF_2)_4$–(CF_2CF_2)]$_m$H ($n = 5m$) and H[$(CH_2CF_2)_5$–(CF_2CF_2)]$_m$H ($n = 6m$), which were designed for different TeFE contents. As those in Ref. [20] for P(VDF–TrFE), the models are for the ideal arrangement of alternating copolymers for simplifying the calculations. This is because the clearly reported alternating piezoelectric copolymer is seen only in vinylidene cyanide with a number of other co-monomers [68,69]. Although the reported piezoelectric P(VDF–TeFE)s are the random copolymers, it is reasonable that there must be a higher proportion of alternating arrangement in the material as our models. In vibration analyses, the exact molecular polarizability tensors, α_{xx}^{mol}, α_{xy}^{mol}, α_{yy}^{mol}, α_{xz}^{mol}, α_{yz}^{mol} and α_{zz}^{mol}, are obtained, in which, e.g. α_{xy}^{mol}, is defined as the linear response to an externally applied electric field [70]: $\mu_x^{ind} = \alpha_{xy}^{mol} E_y^{ext}$, where μ^{ind} is the induced molecular dipole moment, E^{ext} is the magnitude of the applied electric field and x, y, z represent the Cartesian components. In simulating the spectra, the B3PW91/6-31G(d) frequencies were scaled by the scaling factor 0.9573 [71].

3. Results and discussion

3.1. Internal rotation of related dimers

Internal rotation potential is the most important intrinsic property to reflect the conformation distribution of a polymer chain. It is reasonable to examine a dimer model (for convenience) of a polymer chain to emphasize the intramolecular rotation potentials. In the chain of P(VDF–TeFE) copolymer, both H[CH_2CF_2–CF_2CF_2]H (referring as model I) and H[CF_2CH_2–CF_2CF_2]H (referring as model II) dimer models can be drawn, and will be examined. The rotation angle starts and terminates at C–C–C–C *eclipsed*-conformation (denoted as zero and 360° for the C–C–C–C dihedral angle). Newman projections of *eclipsed*, *gauche* and *trans* configurations in P(VDF–TeFE) dimer models (upper panel) and the internal rotation potential curves (lower panel) are shown in Fig. 1(A) in solid circles for model I, and in Fig. 1(B) in circles for model II. Also plotted are the curves of P(VDF–TrFE) from Ref. [20] in Fig. 1(C) in solid triangles for the model of H[CH_2CF_2–$CHFCF_2$]H (referring as I) and from present calculations in Fig. 1(D) in triangles for the model of H[CF_2CH_2–CF_2CHF]H (referring as II), and the curve of the solely existed dimer model of PVDF from Ref. [19] in Fig. 1(E) in stars. The most stable conformations of PVDF (curve (E) at ±55°), P(VDF–TrFE)$_I$ (curve (C) at 290°) and P(VDF–TeFE)$_I$ (curve (A) at ±177°) are plotted with zero energy. The curve for model II is plotted with the energy relative to the respective model I in each system.

It is interesting that the energies of P(VDF–TeFE)$_{II}$ are systematically higher than those of model I. Similar results are seen in P(VDF–TrFE) except the energy barrier in 110–145°. The higher energies are from the different intrinsic structures of the polymer chains and thus the curve for model I or II is actually independent, or the energy differences between I and II will not affect any of the further discussions of the conformation transitions.

Fig. 1(A) and (B) shows that the angles for the g and g' conformations in the α-chain ($tgtg'$) models are ±67° in model I and ±63° in model II. Compared with P(VDF–TrFE) and PVDF, the values are 53° and −70° in P(VDF–TrFE)$_I$, 53° and −65° in P(VDF–TrFE)$_{II}$ and ±55° in PVDF. Therefore, the respective angle in P(VDF–TeFE)$_I$ is 12° larger than that in PVDF [19], 14° larger than the g conformation and 3° smaller than the g' conformation in P(VDF–TrFE)$_I$ [20]. Similarly, the respective angle in P(VDF–TeFE)$_{II}$ is 8° larger than that in PVDF [19], 10° larger than the g conformation and 2° smaller than the g' conformation in P(VDF–TrFE)$_{II}$. Conformation differences between models I and II, and among the different systems can also be found in detail in Fig. 1. On examining the structures of P(VDF–TeFE), it is found that the negative F atoms in different units are in small distances when the conformation angles are small. This leads to larger repulsion, and consequently larger stable angles compared with PVDF and the g conformation in P(VDF–TrFE). However, in PVDF there exist more attractions between the dense pairs of positive H and negative F atoms and result in small stable angles. The β-chain (ttt) conformation is a slightly distorted plane with dihedral angles at ±177° in model I and at ±176° in model II. Similar to PVDF [19], the *all-trans* "ideal β-chain conformation" of P(VDF–TeFE) (with the carbon backbone dihedral angle being 180°) is also a transition state (confirmed by frequencies analysis) in the path of internal rotation with very small energy barrier of about 0.1 kJ/mol. This predicts that the carbon dihedral repeating motif of the β-chain copolymer would also be in an arbitrary angle around and very close to 180°.

The energy differences between the β- and α-conformation are negative values by −0.7 kJ/mol in P(VDF–TeFE)$_I$ and −3.6 kJ/mol in P(VDF–TeFE)$_{II}$. This is different from the positive values of 8.4 kJ/mol in PVDF [19] and, 2.1 (tg) and 7.8 kJ/mol (tg') in P(VDF–TrFE)$_I$ [20]. It must be a desirable property in the interested material that the β-conformation in P(VDF–TeFE) is more stable than the α-conformation thermodynamically. The energy differences in P(VDF–TrFE)$_{II}$ examined presently are −3.3 kJ/mol (tg) and 7.7 kJ/mol (tg') and the results will support and enhance the discussions in our previous work [20].

The energy barriers of the β → α transitions are 12.4 kJ/mol in P(VDF–TeFE)$_I$ and 9.5 kJ/mol in P(VDF–TeFE)$_{II}$.

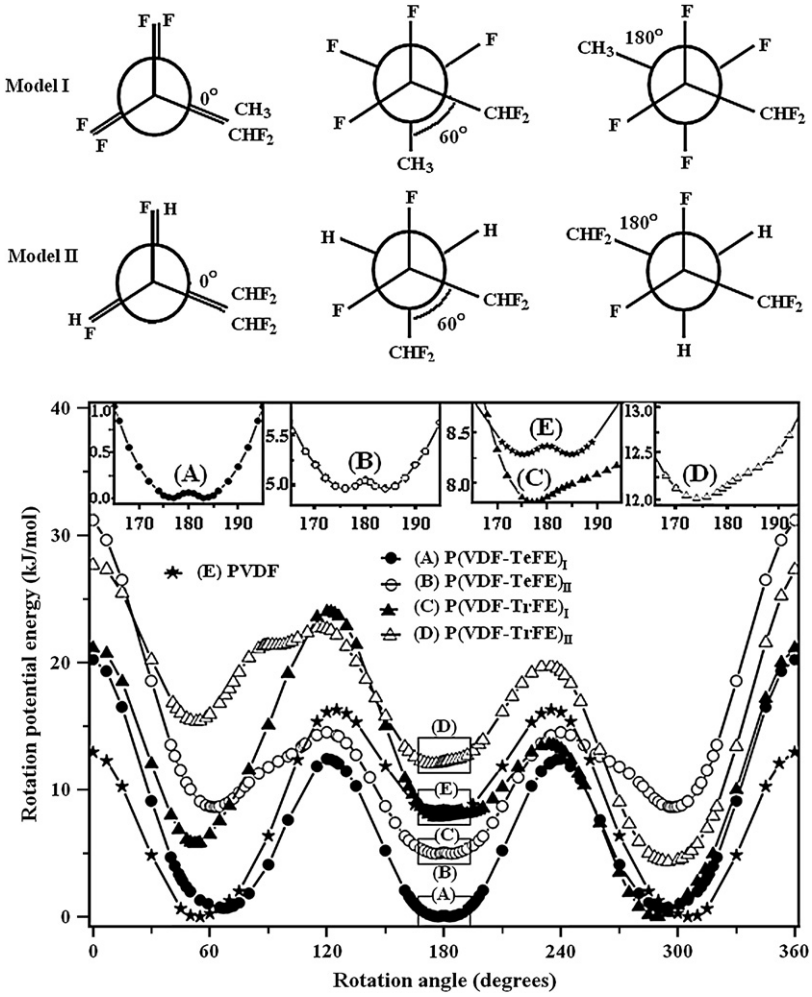

Fig. 1. Newman projections of *eclipsed*, *gauche* and *trans* configurations of P(VDF–TeFE) dimer models (upper panel) and internal rotation potential energy curves of P(VDF–TeFE), P(VDF–TrFE) and PVDF chain models (lower panel): (A) $H(CH_2CF_2)$–$(CF_2CF_2)H$; (B) $H(CF_2CH_2)$–$(CF_2CF_2)H$; (C) $H(CH_2CF_2)$–$(CHFCF_2)H$ (from Ref. [20]); (D) $H(CF_2CH_2)$–$(CF_2CHF)H$ and (E) $H(CH_2CF_2)$–$(CH_2CF_2)H$ (from Ref. [19]) obtained by B3PW91/6-31G(d) calculations.

Both of the values are larger than the barrier, 8.2 kJ/mol, in PVDF [19]. Therefore, the β → α transition in P(VDF–TeFE) is more difficult than that in PVDF once it is formed. This will be a very useful property in practical applications in preventing the piezoelectric phase from depolarization.

Additionally, the same energy barriers found in this work are 10.7 (β → α(g)) and 7.7 kJ/mol (β → α(g')) in $P(VDF–TrFE)_{II}$. Those in Ref. [20] are 16.2 (β → α(g)) and 5.8 kJ/mol (β → α(g')) in $P(VDF–TrFE)_{I}$. These results suggest that the phase transition in P(VDF–TrFE) will be more complex as has been found in the experiments [18,26,38,72–75] and presented in Ref. [20]. However, both of the smaller barriers, 5.8 and 7.7 kJ/mol, are lower than that in P(VDF–TeFE) or PVDF. It is reasonable to predict that the property of depolarization of P(VDF–TrFE) would not be better than either P(VDF–TeFE) or PVDF.

3.2. Structure and stability

For P(VDF–TeFE) copolymers with different TeFE contents, structures of α-($tgtg'$) and β-chain (ttt) within 2–n ($n = 20$ or 21) monomer units in the models of $H[(CH_2CF_2)–(CF_2CF_2)]_mH$ ($n = 2m$), $H[(CH_2CF_2)_2–(CF_2CF_2)]_mH$ ($n = 3m$), $H[(CH_2CF_2)_3–(CF_2CF_2)]_mH$ ($n = 4m$) and $H[(CH_2CF_2)_4–(CF_2CF_2)]_mH$ ($n = 5m$) were optimized and compared with those of PVDF [19] and P(VDF–TrFE) [20]. The corresponding mole ratios of TeFE in these models are 0.50, 0.33, 0.25, 0.20 and 0.17.

The structures optimized at B3PW91/6-31G(d) level for the models with 20 or 21 monomer units are shown in Fig. 2(a)–(h). For the ideal β-conformation copolymers, all of the chains are curved. It is very interesting to note that the β-chain P(VDF–TeFE)s containing different TeFE contents have almost identical curvature radii by 29 ~ 30 Å (Fig. 2(a), (c), (e), (g)), extremely similar to the values in both β-PVDF homopolymer [19] and β-P(VDF–TrFE) copolymers [20]. As that in the β-P(VDF–TrFE) copolymers [20], this is also an unexpected result since it would be expected that increase of the ratio of TeFE (having more F atoms to balance the number of F atoms on both sides of the chain axis) would have reduced the curvature of β-chains. However, it remains almost unchanged. In fact, the chains with enriched F atoms have

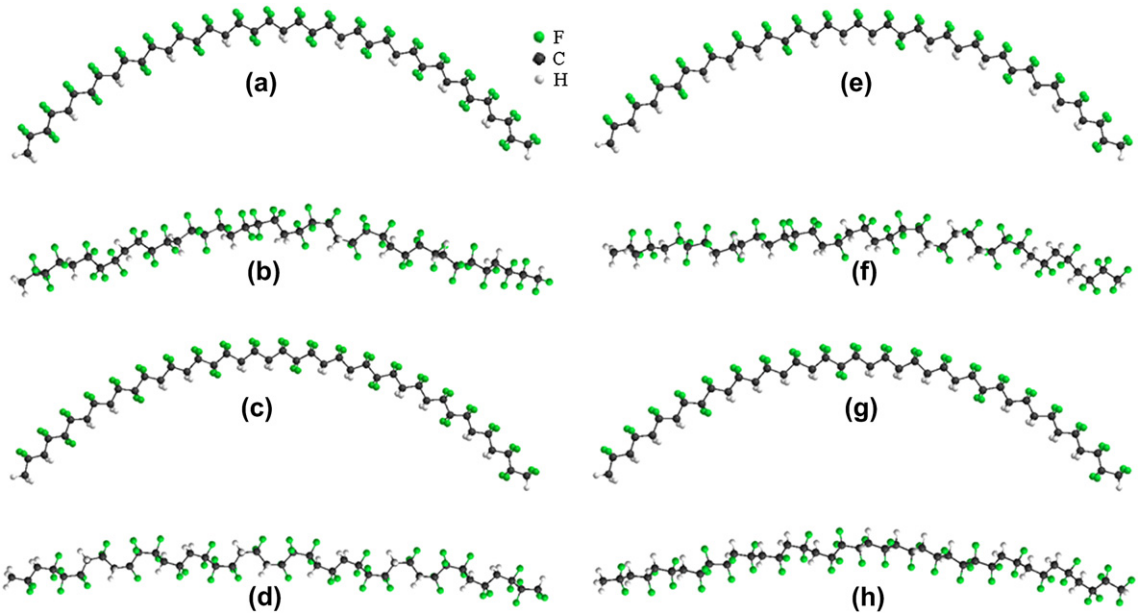

Fig. 2. Structures of P(VDF–TeFE) optimized by B3PW91/6-31G(d) calculations: (a) and (b) are for β- and α-chain with 20 monomers containing 0.50 mole fraction of TeFE in $H[(CH_2CF_2)–(CF_2CF_2)]_mH$; (c) and (d) are for β- and α-chain with 21 monomers containing 0.33 mole fraction of TeFE in $H[(CH_2CF_2)_2–(CF_2CF_2)]_mH$; (e) and (f) are for β- and α-chain with 20 monomers containing 0.25 mole fraction of TeFE in $H[(CH_2CF_2)_3–(CF_2CF_2)]_mH$; (g) and (h) are for β- and α-chains with 20 monomers containing 0.20 mole fraction of TeFE in $H[(CH_2CF_2)_4–(CF_2CF_2)]_mH$.

slightly smaller average (in 6–20/21 chain units) curvature radii by 28.81, 29.51, 29.64 and 29.70 Å for the models containing 0.50, 0.33, 0.25 and 0.20 mole fractions of TeFE, respectively. The values are 30.31 Å in PVDF and 29.10–29.83 Å in P(VDF–TrFE). As has been presented in Ref. [20], the explanation of the over-all smaller radius is that the pairs of alternate electrostatic attraction (between the negative F atom and the neighboring positive H atom) increases as shown in Fig. 2(a). The smaller chain-curving for the smaller TeFE ratio chains is understandable by electrostatic interactions as what in P(VDF–TrFE) [20], i.e. there is less electrostatic attraction on the inner side of the chain with less F atom couples and H atom couples, and consequently the radius is the largest by 29.70 Å for the copolymer with 0.20 mole fraction of TeFE. It should be noted that the similar curving in these different systems must be an occasional coincidence.

Compared with the arched planar α-PVDF homopolymer [19], α-P(VDF–TeFE) copolymer chain containing 0.50 mole fraction of TeFE is also *helical* chain structure (Fig. 2(b)) as P(VDF–TrFE) with the same VDF content [20]. This result agrees well with the observation of X-ray diffraction [16]. The chains with 0.33 (Fig. 2(d)), 0.25 (Fig. 2(f)) and 0.20 (Fig. 2(h)) mole fractions of TeFE are nearly in straight line, but not as straight as the P(VDF–TrFE) chains with same VDF contents [20]. In fact, the optimized structures show that the *helical*-pitch of the α-P(VDF–TeFE) chains increase with decreasing TeFE contents. Therefore, the chains with low TeFE may be viewed almost as a straight line in the reached model lengths of this work. This behavior is similar to P(VDF–TrFE) with similar VDF contents observed by neutron diffraction [76] and predicted theoretically by DFT [20]. Thus higher TeFE content would lead the α-P(VDF–TeFE) chains to twist more and be in favor of forming the *helical* structure. This is reasonable since the conformation even in the pure polytetrafluoroethy1ene (PTFE) is always a slightly twisted *helix* [77–79], leading to semicrystalline PTFE bulk material (crystalline, amorphous and quasi-ordered mixture [80]). Beall et al. [81] have also observed that increasing the steric hindrance (implying increasing atactic degree) of polymer chain will increase the free volume in the fluorine polymers. Therefore, P(VDF–TeFE) in the form of the nearly straight linear α-chain (with low TeFE content) will have higher crystallinity, which is helpful for electro-processing the polymer into the satisfactory piezoelectric β-phase.

To explore the variation of the relative stability of the α- and β-chain at different TeFE contents, the energy difference per monomer unit, $(E_\beta - E_\alpha)/n$, between the β- and α-chain P(VDF–TeFE) with different mole ratios of TeFE and the chain lengths were examined and compared with those of PVDF. Fig. 3(a) shows the energy difference of PVDF [19] homopolymer for comparison. Fig. 3(b)–(f) plots the energy differences, i.e. $((E_\beta - E_\alpha)/n)$ *vs.* chain length n ($2 \leq n \leq 20$). The contents of TeFE in Fig. 3(b)–(f) are 0.50, 0.33, 0.25, 0.20 and 0.17 (mole fraction), respectively.

The figure shows that the energy difference in the copolymer with a constant TeFE content also slightly increases and converges to a nearly constant value with increasing chain length for $n \geq 5$ (Fig. 3(b)–(f)) as that seen in PVDF (Fig. 3(a)) [19]. However, all of the values shown in Table 1 (1.4–5.8 kJ/mol) are smaller than that (10 kJ/mol) in PVDF [19] and those (4.1–8.3 kJ/mol) in P(VDF–TrFE)s [20]. It is also shown that the energy differences increase with decreasing TeFE content. The results indicate that the

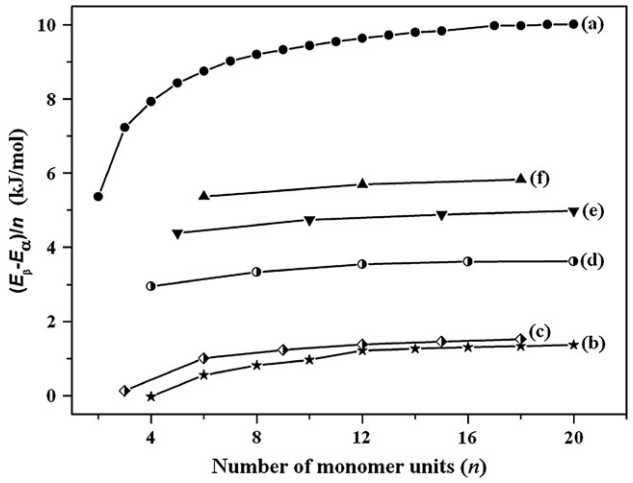

Fig. 3. Energy difference ($(E_\beta - E_\alpha)/n$ *vs.* chain length) per monomer unit between the β- and α-chain obtained from B3PW91/6-31G(d) calculations: (a) PVDF homopolymer from Ref. [19]; (b) 0.50 mole fraction of TeFE in P(VDF−TeFE), H[(CH_2CF_2)−$(CF_2CF_2)]_m$H ($n = 2m$); (c) 0.33 mole fraction of TeFE in P(VDF−TeFE), H[$(CH_2CF_2)_2$−$(CF_2CF_2)]_m$H ($n = 3m$); (d) 0.25 mole fraction of TeFE in P(VDF−TeFE), H[$(CH_2CF_2)_3$−$(CF_2CF_2)]_m$H ($n = 4m$); (e) 0.20 mole fraction of TeFE in P(VDF−TeFE), H[$(CH_2CF_2)_4$−$(CF_2CF_2)]_m$H ($n = 5m$) and (f) 0.17 mole fraction of TeFE in P(VDF−TeFE), H[$(CH_2CF_2)_5$−$(CF_2CF_2)]_m$H ($n = 6m$).

introduction of TeFE units enhances the relative stability of the β-chain copolymer. This is helpful to understand why the copolymers would contain at least 0.07 mole fraction of TeFE [29] to crystallize with the *all-trans* conformation of the ferroelectric β-phase. Although the relative stability of β-chain increases with increasing TeFE content, the tacticity of the α-chain decreases with increasing TeFE content (e.g. the *helical* structure appears in the chain of 0.50 mole fraction TeFE). Therefore, an optimized composition should exist in P(VDF−TeFE)s for crystallinity (or electrical properties).

Table 1
Magnitudes of the energy difference per monomer unit between the β- and α-chain for different VDF contents (in mole fractions) in P(VDF−TeFE) copolymer and the contribution magnitude of average dipole moment per monomer unit in the β-chain P(VDF−TeFE) with 15 and 20 monomer units and with different VDF contents obtained from B3PW91/6-31G(d) calculations

VDF content in the P(VDF−TeFE)/mole fractions	0.50[a]	0.67[b]	0.75[c]	0.80[d]	0.83[e]	1.00[f]
Energy differences per monomer unit $(E_\beta - E_\alpha)/n$, kJ/mol	1.4	1.5	3.6	5.0	5.8	10.0
Average dipole moment per monomer unit[g]/10^{-30} C m	2.65	3.53	3.95	4.22	4.39	5.31
Average dipole moment per monomer unit[h]/10^{-30} C m	2.47	3.32	3.73	4.00	4.18	5.10

[a] P(VDF−TeFE), H−[(CH_2CF_2)−$(CF_2CF_2)]_m$−H.
[b] P(VDF−TeFE), H−[$(CH_2CF_2)_2$−$(CF_2CF_2)]_m$−H.
[c] P(VDF−TeFE), H−[$(CH_2CF_2)_3$−$(CF_2CF_2)]_m$−H.
[d] P(VDF−TeFE), H−[$(CH_2CF_2)_4$−$(CF_2CF_2)]_m$−H.
[e] P(VDF−TeFE), H−[$(CH_2CF_2)_5$−$(CF_2CF_2)]_m$−H.
[f] PVDF H−[$(CH_2$−$CF_2)_n$]−H, homopolymer.
[g] Chains with 15 monomer units, data are derived from Fig. 4.
[h] Chains with 20 monomer units, data are derived from Fig. 4.

3.3. Dipole moment and mean polarizability

The average permanent dipole moment per monomer unit $\mu = (\mu_x^2 + \mu_y^2 + \mu_z^2)^{1/2}/n$ is shown in Fig. 4 and the dependence of contributed magnitude of average dipole moment per monomer unit on VDF content in the β-chain P(VDF−TeFE) is shown Fig. 5. The mean polarizabilities per monomer unit $\alpha = (\alpha_{xx} + \alpha_{yy} + \alpha_{zz})/3n$ [69] for different chain lengths (n units) and different VDF contents are shown in Fig. 6.

For the α-chain P(VDF−TeFE)s, Fig. 4(d), (f), (h), (j) and (l) shows that the over-all average dipole moment contribution per monomer unit decreases with increasing chain length. It is interesting that the average dipole moment contribution per monomer unit of the α-chain P(VDF−TeFE) containing 0.5 mole fraction of TeFE (Fig. 4(d)) is higher than the corresponding β-chain (Fig. 4(c)) if the chain length n is less than seven. This is mainly due to the contribution of the dipole moment not being zero in the *gauche*-conformation of −(CF_2CF_2)− but being exactly zero in the *all-trans* conformation.

Similar to that in β-PVDF [19], the average dipole moment contribution per monomer unit decreases with increasing chain length for the β-chain P(VDF−TeFE)s (Fig. 4(c), (e), (g), (i) and (k)). This is because the dipole moment in the individual monomer unit is perpendicular to the chain axis but the β-chain P(VDF−TeFE)s are curved. The decreased magnitude, −1.18%, of average dipole moment contribution per monomer unit is similar to that of PVDF (−1.2% [19]) and that of P(VDF−TrFE) (−1.24% [20]). The result is consistent with the fact that P(VDF−TeFE)s have similar curvature radii (28.8∼29.70 Å) as the values (∼30 Å) in β-chain PVDF [19] and P(VDF−TrFE)s [20] discussed previously. Similar to P(VDF−TrFE) copolymers [20], the absolute value of the dipole moment decreased in P(VDF−TeFE)s with higher

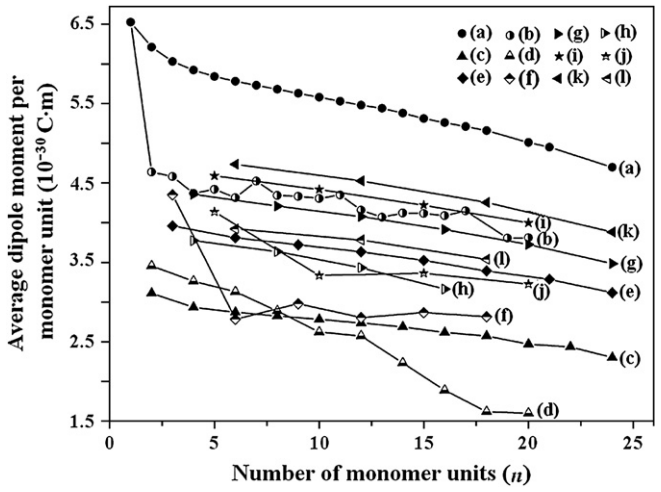

Fig. 4. Average dipole moment per monomer unit *vs.* P(VDF−TeFE) chain length: (a) and (b) are for β- and α-chain PVDFs from Ref. [19]; (c) and (d) are for β- and α-chain P(VDF−TeFE)s containing 0.50 mole fraction of TeFE; (e) and (f) are for β- and α-chain P(VDF−TeFE)s containing 0.33 mole fraction of TeFE; (g) and (h) are for β- and α-chain P(VDF−TeFE)s containing 0.25 mole fraction of TeFE; (i) and (j) are for β- and α-chain P(VDF−TeFE)s containing 0.20 mole fraction of TeFE; (k) and (l) are for β- and α-chain P(VDF−TeFE)s containing 0.17 mole fraction of TeFE.

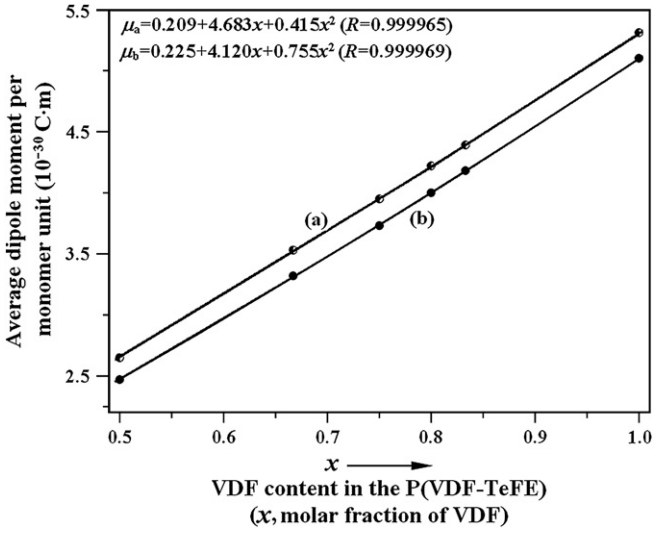

Fig. 5. Dependence of contributed magnitude of average dipole moment per monomer unit on VDF content in the β-chain P(VDF–TeFE) obtained from B3PW91/6-31G(d): (a) 15 monomer units and (b) 20 monomer units.

TeFE content. This is because the $-(CF_2CF_2)-$ monomer with β-conformation in TeFE has zero dipole moment. For the β-chain copolymer with 15 and 20 monomer units, the results are listed in Table 1.

For the β-chain P(VDF–TeFE) containing two units, [i.e. $H(CH_2CF_2-CF_2CF_2)H$], the contribution magnitude of average dipole moment is 3.11×10^{-30} C m as shown in Fig. 4(c) if the chain curvature can be neglected, which is consistent with the prediction of *ab initio* multigrid-based total-energy method ($(2.0 + 0.0)/2$ Debye $= 3.34 \times 10^{-30}$ C m)[14]. Although the contribution magnitude of the average dipole moment per monomer unit decreases with increasing the chain length, the total dipole moment increases with increasing the chain length.

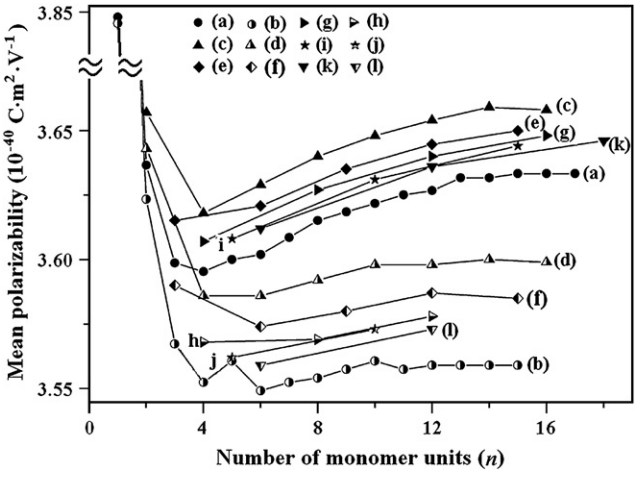

Fig. 6. Mean polarizability per monomer unit *vs*. length of the copolymer chains: (a) and (b) are for β- and α-chain PVDF from Ref. [19]; (c) and (d) are for β- and α-chain P(VDF–TeFE)s containing 0.50 mole fraction of TeFE; (e) and (f) are for β- and α-chain P(VDF–TeFE)s containing 0.33 mole fraction of TeFE; (g) and (h) are for β- and α-chain P(VDF–TeFE)s containing 0.25 mole fraction of TeFE; (i) and (j) are for β- and α-chain P(VDF–TeFE)s containing 0.20 mole fraction of TeFE; (k) and (l) are for β- and α-chain P(VDF–TeFE)s containing 0.17 mole fraction of TeFE.

For the copolymer chains with 10 and 20 monomers, for example, the values (in 10^{-30} C m) are 27.8 and 49.4 (with 0.50 mole fraction of TeFE), 39.6 and 66.4 (with 0.33 mole fraction of TeFE), 41.5 and 74.5 (with 0.25 mole fraction of TeFE), 44.2 and 80.0 (with 0.20 mole fraction of TeFE), and 45.9 and 83.0 (with 0.17 mole fraction of TeFE). Therefore, β-P(VDF–TeFE) copolymer with longer chain and with lower TeFE content has higher piezoelectric and pyroelectric properties.

The magnitude of average dipole moment per monomer unit contributed in β-P(VDF–TeFE) with 15 and 20 monomer units versus the VDF content (in mole fraction) is plotted in Fig. 5. The figure shows that the average dipole moment per monomer unit increases rapidly with increasing VDF content (or decreases with increasing TeFE). This is because the dipole moment in TeFE is exactly zero. The curve is nearly a straight line, but still there exists a very weakly parabolic dependence. This result is similar to those predicted by *ab initio* multigrid-based total-energy method [14] in P(VDF–TrFE) and P(VDF–TeFE) copolymers. As has been proposed in Ref. [14], a fit to the curves may provide an estimation of the contribution magnitude of average dipole moment (in 10^{-30} C m) per monomer unit in the β-chain P(VDF–TeFE)s (with 15 and 20 monomer units) at any VDF mole fraction x in the range between $0.50 \sim 1.00$. Both of the linear and quadratic equations are (with the correspondence correlation coefficient R in the parentheses):

$$\mu_{(15\ \text{monomers})} = -0.013 + 5.303x \quad (R = 0.99987)$$

$$\mu_{(20\ \text{monomers})} = -0.178 + 5.245x \quad (R = 0.99963)$$

$$\mu_{(15\ \text{monomers})} = 0.209 + 4.683x + 0.415x^2 \quad (R = 0.99996)$$

$$\mu_{(20\ \text{monomers})} = 0.225 + 4.119x + 0.755x^2 \quad (R = 0.99997)$$

The quadratic fit is slightly better than the linear. The reason for the very weakly parabolic dependence is the same as in P(VDF–TrFE) [20], which is due to the curvature of the chain slightly decreased with increasing VDF content (as discussed in Section 3.2) that leads to the average dipole moment contribution increased slightly.

Fig. 6 shows that the mean polarizability per monomer unit in the β-chain P(VDF–TeFE) is slightly higher than that in the α-chain. Chain length does not significantly affect the mean polarizability of either α- or β-P(VDF–TeFE). For β-chain P(VDF–TeFE)s with different VDF contents, the mean polarizabilities per monomer unit are in a small range of $3.63-3.66 \times 10^{-40}$ C m^2 V^{-1}. The sequence in the models is $0.50 > 0.33 > 0.25 > 0.20 > 0.17$ (mole fraction of TeFE). The same sequence is also found in α-chain P(VDF–TeFE) with the mean polarizabilities in the range of $3.60-3.56 \times 10^{-40}$ C m^2 V^{-1}.

3.4. Vibrational spectra

The infrared spectrum must be one of the most important tools to examine the properties associated with the changes

of the chain composition and chain conformation of a copolymer. The spectra for both α- and β-chain P(VDF–TeFE)s, with 5 through 15 monomer units containing different TeFE contents (0.50, 0.33, 0.25, 0.20, 0.17 and 0.14 mole fractions of TeFE) were calculated. Some of the results within the wave number 400–1500 cm^{-1} are shown in Figs. 7 and 8. Fig. 7(a) is the simulated spectra of the α-chain PVDF homopolymer having 15 monomer units [19] as a reference, Fig. 7(b)–(e) are for α-chain P(VDF–TeFE) copolymers having 12 or 14 or 15 monomer units with different TeFE contents. Fig. 8(a) is the simulated spectra of β-chain PVDF having 15 monomer units for comparison [19], Fig. 8(b)–(e) are for β-chain P(VDF–TeFE)s having 12 or 14 or 15 monomer units with different TeFE contents.

Comparison shows that the spectra of α-chain P(VDF–TeFE) copolymers with different TeFE contents are similar to the spectra of the α-chain PVDF homopolymer [19] (Fig. 7(a)). The most distinguishable vibrational modes are found at peaks 1321 (C–H rocking), 921 ($-CH_2$ rocking) and 628 cm^{-1} ($-CH_2$ rocking and skeletal bending) (Fig. 7(b)), which did not appear in the homopolymer PVDF. The peak at 1321 cm^{-1} is quite weak in intensity but is obviously visible. The position changes slightly within ±5 cm^{-1} in different TeFE contents. The peak at 921 cm^{-1} has a medium intensity. The position is almost unchanged in the copolymer having 0.20–0.33 mole fraction of TeFE (Fig. 7(b)–(d)) but shifts to 943 cm^{-1} in the copolymer with 0.50 mole fraction of TeFE (Fig. 7(e)). The peak at 628 cm^{-1} also has a medium intensity and the position shifts to higher wave numbers, i.e. 628, 637 and 639 cm^{-1} in the copolymers containing 0.20, 0.25 and 0.33 mole fractions of TeFE, respectively. However, in the copolymer with 0.50 mole fraction of TeFE (Fig. 7(e)) the intensity increases but the position remains almost unchanged at 627 cm^{-1}. Other peaks that exist in both PVDF homopolymer and P(VDF–TeFE) copolymers are also distinguishable. The intensity of the peak at 877 cm^{-1} ($-CH_2$ rocking) decreases with increasing TeFE content and the frequency of α-PVDF at 470 cm^{-1} (CH_2 rocking and skeletal bending) shifts to higher wave numbers (i.e. from 470 to 490 cm^{-1}) in the α-P(VDF–TeFE). The intensity of the 470 cm^{-1} peak increases with increasing TeFE content. These characteristics must be useful references for further identification of the polymers.

Fig. 8 shows the simulated IR spectra of β-chain P(VDF–TeFE)s with different TeFE contents. The spectra are also similar to those of β-chain PVDF [19] (Fig. 8(a)). The most distinguishable vibrational modes are found at peaks 1289, 1138, 839 and 430–442 cm^{-1}. The intensity of the peak at 1289 cm^{-1} decreases and the position shifts to higher wave numbers [i.e. from 1289 in PVDF (Fig. 8(a)) to 1317 cm^{-1} in P(VDF–TeFE) containing 0.50 mole fraction of TeFE (Fig. 8(e))] with increasing TeFE contents. A fit to the curves may also provide an estimation of the peak position and relative intensity (I/I_{max}) of β-copolymer with different TeFE contents at any TeFE mole fraction x in the range of 0.50–0.14. The linear equations of the peak position and relative intensity are (with the correlation coefficient R in the parentheses):

$$1289\text{-peak position} = 1294.4 + 46.4x\ cm^{-1} \quad (R = 0.9935)$$

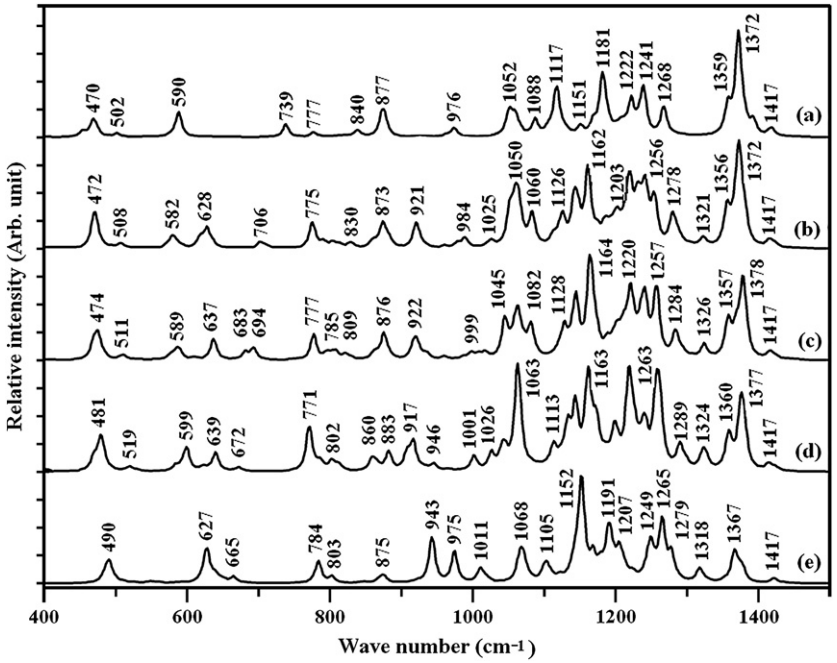

Fig. 7. Comparison of the IR spectra of α-chain P(VDF–TeFE)s with different TeFE contents obtained from B3PW91/6-31G(d) calculations: (a) PVDF with 15 monomer units (from Ref. [19], where the labeled theoretical wavenumbers had not been scaled by the scaling factor 0.9573, which is not consistent with the text of that paper. The present labels are the scaled values.); (b) P(VDF–TeFE) with 15 monomer units containing 0.20 mole fraction of TeFE; (c) P(VDF–TeFE) with 12 monomer units containing 0.25 mole fraction of TeFE; (d) P(VDF–TeFE) with 15 monomer units containing 0.33 mole fraction of TeFE; (e) P(VDF–TeFE) with 14 monomer units containing 0.50 mole fraction of TeFE. All of the labeled frequencies were scaled by the scaling factor 0.9573 from Ref. [71].

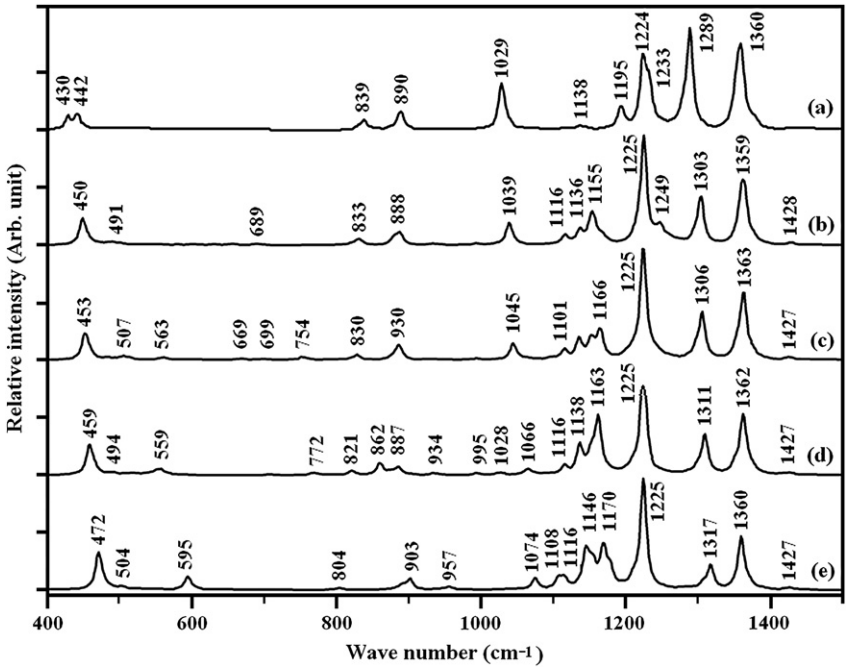

Fig. 8. Simulated IR spectra of β-chain P(VDF−TeFE) and PVDF from B3PW91/6-31G(d) calculations: (a) PVDF with 15 monomer units from Ref. [19]; (b) P(VDF−TeFE) with 15 monomer units containing 0.20 mole fraction of TeFE; (c) P(VDF−TeFE) with 12 monomer units containing 0.25 mole fraction of TeFE; (d) P(VDF−TeFE) with 15 monomer units containing 0.33 mole fraction of TeFE and (e) P(VDF−TeFE) with 14 monomer units containing 0.50 mole fraction of TeFE. All of the labeled frequencies were scaled by the scaling factor 0.9573 from Ref. [71].

$$I/I_{\max}(1289) = 0.9552 - 0.7606x \quad (R = 0.9994)$$

The mode corresponds to all of the C^F (where C^F refers to the C atom bonding F atoms) atoms symmetrically (perpendicular to the chain axis) in-plane stretching. The intensity of the band at 1138 cm^{-1} (CH_2 rocking) increases dramatically and the peaks split as well as broaden with increasing TeFE content. This is quite different from the peak in PVDF homopolymer with very weak (almost invisible) intensities. The intensity of the characteristic vibrational peak of β-PVDF at 839 cm^{-1} (all of the $-CH_2$ groups collectively and symmetrically moving in-plane and perpendicular to the polymer chain axis [19]) decreases and the position shifts to lower frequencies (839 → 833 → 830 → 821 → 804 cm^{-1}) with increasing TeFE content. The linear fit equations for the peak position and relative intensity with x (also TeFE mole fraction) in the range of 0.50−0.14 are:

$$839\text{-peak position} = 852.8 - 95.6x\ cm^{-1} \quad (R = 0.9982)$$

$$I/I_{\max}(839) = 0.0657 - 0.103x \quad (R = 0.9995)$$

The theoretical results are consistent with the experimental observations [36], where the peak positions are 842, 839 and 820 cm^{-1} for copolymers with VDF 81%, 75% and 64%/TeFE. The intensity of the peak at 1360 cm^{-1} increases with increasing VDF content and this is also consistent with the experimental observations [37]. The split peaks at 430 and 442 cm^{-1} (C−C skeletal bending) in PVDF merged into one in the copolymers. The intensity increases and the position shifts to higher wave numbers [i.e. from 430−442 cm^{-1} in PVDF (Fig. 8(a)) to 472 cm^{-1} in the P(VDF−TeFE) containing 0.50 mole fraction of TeFE (Fig. 8(e))]. These results are also useful for identification of β-P(VDF−TeFE)s containing different TeFE.

4. Conclusions

DFT-B3PW91/6-31G(d) has been employed to investigate the internal rotation potentials, geometries, relative stabilities, vibrational spectra, dipole moments and mean polarizabilities of the α- and β-chain P(VDF−TeFE) with different TeFE contents. Influences of chain length and TeFE (or VDF) content on the stabilities, chain conformation, electric properties and vibrational spectra have been examined. The following conclusions are drawn.

1. Conformation angles in the α-chain (*tgtg′*) dimer models (H[CH_2CF_2−CF_2CF_2]H and H[CF_2CH_2−CF_2CF_2]H) are ±67° and ±63°, which are different from +53° and −70° in P(VDF−TrFE) and ±55° in PVDF. The β-chain (*ttt*) conformations are in a slightly distorted *all-trans* plane with dihedral angles at ±177° and ±176°. This is closer to the ideal β-conformation compared with PVDF (±175°).

   The energy differences between the β- and the α-conformation in both the dimer models are negative values by −0.7 or −3.6 kJ/mol compared with the positive one (8.4 kJ/mol) in PVDF, and those by 2.1 or −3.3 (β → *g*) and by 7.8 or 7.7 kJ/mol (β → *g′*) in P(VDF−TrFE) (in the model of H[CH_2CF_2−$CHFCF_2$]H or H[CF_2CH_2−CF_2CHF]H). These results show that the β-conformation

in P(VDF–TeFE) copolymer should be more stable than that in PVDF and most of those in P(VDF–TrFE) thermodynamically. The result is consistent with the experimental fact that the copolymers may crystallize directly from the melting state into a piezoelectric crystal phase.

The transition energy barrier of the $\beta \rightarrow \alpha$ is 12.4 or 9.5 kJ/mol compared with 8.2 kJ/mol in PVDF and 16.2 or 10.7 ($\beta \rightarrow \alpha(g)$) and 5.8 or 7.7 kJ/mol ($\beta \rightarrow \alpha(g')$) in P(VDF–TrFE). This shows that the $\beta \rightarrow \alpha$ transition in P(VDF–TeFE) is more difficult than that in PVDF. Therefore, the copolymer should be in favor of preventing the piezoelectric phase from depolarization.

2. The ideal β-chains are curved with a radius of about 30 Å, which is very close to those in both PVDF and P(VDF–TrFE). Similar to P(VDF–TrFE), the α-chain containing 0.50 mole fraction of TeFE is also a *helical* structure. However, the α-chains with 0.33–0.20 mole fraction of TeFE are nearly linear in structure, but the chain is not as straight as that in P(VDF–TrFE) with the same VDF content.
3. The energy difference per monomer unit between the β- and α-chain decreases with increasing TeFE content, implying that the introduction of TeFE would enhance the relative stability of the β-chain conformation compared with the pristine homopolymer. This is helpful to understand the experimental fact that why the copolymers need to have at least 0.07 mole fraction of TeFE to crystallize into the *all-trans* conformation (or ferroelectric β-phase).
4. The contribution of average dipole moment per monomer unit in the β-chain is affected by chain curvature and by TeFE content. The chain length and TeFE content will not significantly affect the mean polarizability per monomer unit. For a given chain length of P(VDF–TeFE), a weakly parabolic dependence of the average dipole moment per monomer unit on VDF content is obtained and explained. Chain length does not significantly change the mean polarizability of α- and β-chain P(VDF–TeFE)s. The mean polarizability per monomer unit in the β-chain is slightly higher than that in the α-chain.
5. By comparing the calculated IR spectra of the copolymers with different amount of TeFE and with the experimental data, some of the distinguishable vibrational peaks for α- and β-P(VDF–TeFE) identifications are proposed. Three peaks (1321, 921 and 628 cm^{-1}) that existed only in the α-chain copolymers are found. Peak intensity and position changes for the 877 and 470 cm^{-1} peaks are also obtained. The peaks (or bands) at 1289, 1138, 839 and 430–442 cm^{-1} are identified for β-copolymer characteristics. Linear relationships on the peak position and the relative intensity (I/I_{max}) with respect to TeFE content (in mole fraction x in the range of 0.50–0.14) for the peaks at 1289 and 839 cm^{-1} are presented.

Acknowledgments

This work was supported by the National Nature Science Foundation (No. 50572089 and 50672075) and the Xi'an S and T Research Foundation (GG05015, GG06023). Part of the calculations was performed in the High Performance Computing Center of Northwestern Polytechnical University.

References

[1] Kawai H. Jpn J Appl Phys 1969;8:975–6.
[2] Bergman Jr JG, McFee JH, Crane GR. Appl Phys Lett 1971;18:203–5.
[3] Anderson RA, Kepler RG, Lagasse RR. Ferroelectrics 1981;33:91–4.
[4] Furukawa T, Date M, Fukada E. J Appl Phys 1980;51:1135–41.
[5] Tashiro K, Kobayashi M. Macromolecules 1988;21:2463–9.
[6] Tashiro K, Kobayashi M. Macromolecules 1990;23:2802–6.
[7] Lovinger AJ. Macromolecules 1985;18:910–8.
[8] Furukawa T, Seo N. Jpn J Appl Phys 1990;29:675–80.
[9] Yuki T, Ito S, Koda T, Ikeda S. Jpn J Appl Phys 1998;37:5372–4.
[10] Chung MY, Lee DC. J Korean Phys Soc 2001;38:117–22.
[11] Kepler RG, Anderson RA, Lagasse RR. Phys Rev Lett 1982;48:1274–7.
[12] Yagi T, Tatemoto M, Sako JI. Polym J 1980;12:209–23.
[13] Higashihata Y, Sako J, Yagi T. Ferroelectrics 1981;32:85–92.
[14] Nakhmanson SM, Buongiorno Nardelli M, Bernholc J. Phys Rev B 2005;72:115210.
[15] Hicks JC, Jones TE, Logan JC. J Appl Phys 1978;49:6092–6.
[16] Lovinger AJ. Macromolecules 1983;16:1529–34.
[17] Tajitsu T, Chiba A, Furukawa T, Date M, Fukada E. Appl Phys Lett 1980;36:286–8.
[18] Tashiro K, Takano K, Kobayashi M, Chatani Y, Tadokoro H. Polymer 1981;22:1312–4.
[19] Wang ZY, Fan HQ, Su KH, Wen ZY. Polymer 2006;47:7988–96.
[20] Wang ZY, Fan HQ, Su KH, Wang Xin, Wen ZY. Polymer 2007;48:3226–36.
[21] Furukawa T. IEEE Trans Electr Insul 1989;24:375–94.
[22] Tajitsu Y, Ogura H, Chiba A, Furukawa T. Jpn J Appl Phys Part 1 1987;26:554–60.
[23] Tasaka S, Miyata S. J Appl Phys 1985;57:906–10.
[24] Ohigashi H, Omote K, Gomyo T. Appl Phys Lett 1995;66:3281–3.
[25] Omote K, Ohigashi H, Koga K. J Appl Phys 1997;81:2760–9.
[26] Tashiro K. Crystal structure and phase transition of PVDF and related copolymers. In: Nalwa HS, editor. Ferroelectric polymers, series of plastic engineering. New York: Marcel Dekker; 1995.
[27] Lovinger AJ. Science 1983;220:1115–21.
[28] Lovinger AJ, Davis DD, Cais RE, Kometani JM. Macromolecules 1988;21:78–83.
[29] Lando JB, Doll WW. J Macromol Sci Phys 1968;2:205–33.
[30] Kochervinskij VV, Glukhov VA, Sokolov VG, Lokshin BV. Vysokomol Soedin Ser A 1989;31:282–8.
[31] Kochervinskij VV, Romadin VF, Glukhov VA, Sokolov VG, Saidakhmetov MA. Vysokomol Soedin Ser A 1989;31:1382–8.
[32] Kochervinskij VV, Glukhov VA, Kuznetsova SYu. Vysokomol Soedin Ser A 1987;29:1530–6.
[33] Latour M. Polymer 1977;18:278–80.
[34] Broadhurst MG, Davis GT, DeReggi AS, Roth SC, Collins RE. Polymer 1982;23:22–8.
[35] Baise AI, Lee BH, Salomon RE, Labes MM. Appl Phys Lett 1975;26:428–30.
[36] Tashiro K, Kaito H, Kobayashi M. Polymer 1992;33(14):2915–28.
[37] Tashiro K, Kaito H, Kobayashi M. Polymer 1992;33(14):2929–33.
[38] Tashiro K, Takano K, Kobayashi M, Chatani Y, Tadokoro H. Ferroelectrics 1984;57:297–326.
[39] Lovinger AJ, Johnson GE, Báir HE, Anderson EW. J Appl Phys 1984;56:2412–8.
[40] Green J, Rabolt JF. Macromolecules 1987;20:456–7.
[41] Murata Y, Koizumi N. Polym J 1985;17:1071–4.
[42] Farmer BL, Hopfinger AJ, Lando JB. J Appl Phys 1972;43:4293–303.
[43] Balta Calleja FJ, Arche AG, Ezquerra TA, Cruz CS, Batallan F, Frick B, et al. Adv Polym Sci 1993;108:1–48.
[44] Ohigashi H, Akama S, Koga K. Jpn J Appl Phys 1988;27:2144–50.

[45] Grozema FC, Candeias LP, Swart M, Van Duijnen PTh, Wildemen J, Hadziioanou G, et al. J Chem Phys 2002;117(24):11366–78.
[46] Hutchison GR, Ratner MA, Marks TJ. J Phys Chem B 2005;109(8):3126–38.
[47] Zhang JP, Frenking G. J Phys Chem A 2004;108:10296–301.
[48] Grozema FC, van Duijnen PT, Siebbeles LDA, Goossens A, de Leeuw SW. J Phys Chem B 2004;108(41):16139–46.
[49] Fratiloiu S, Grozema FC, Siebbeles LDA. J Phys Chem B 2005;109:5644–52.
[50] Zhan CG, Nichols JA, Dixon DA. J Phys Chem A 2003;107(20): 4184–95.
[51] Hutter J, Luthi HP, Diederich F. J Am Chem Soc 1994;116:750–6.
[52] Kwon O, McKee ML. J Phys Chem A 2000;104:7106–12.
[53] Briére JF, Côté M. J Phys Chem B 2004;108:3123–9.
[54] Li FF, Wu DS, Lan YZ, Shen J, Huang SP, Cheng WD, et al. Polymer 2006;47:1749–54.
[55] Yang L, Feng JK, Ren AM, Sun JZ. Polymer 2006;47:1397–404.
[56] Yang L, Feng JK, Ren AM, Sun CC. Polymer 2006;47:3229–39.
[57] Li Y, Feng JK, Liao Y, Ren AM. Polymer 2005;46:9955–64.
[58] Oyman ZO, Ming W, Linde R van der, Gorkum R van, Bouwman E. Polymer 2005;46:1731–8.
[59] Pereira RP, Felishberti MI, Rocco AM. Polymer 2006;47:1414–22.
[60] Yang L, Feng JK, Ren AM. Polymer 2005;46:10970–81.
[61] Mabrouk A, Alimi K, Hamidi M, Bouachrine M, Molinie P. Polymer 2005;46:9928–40.
[62] Su KH, Wei J, Hu XL, Yue H, Lü L. Acta Phys Chim Sin 2000;16: 643–51.
[63] Su KH, Wei J, Hu XL, Yue H, Lü L. Acta Phys Chim Sin 2000;16: 718–23.
[64] Becke AD. J Chem Phys 1992;97:9173–7.
[65] Becke AD. J Chem Phys 1993;98:5648–54.
[66] Burke K, Perdew JP, Wang Y. In: Dobson JF, Vignale G, Das MP, editors. Electronic density functional theory: recent progress and new directions. Plenum; 1998. p. 177–97.
[67] Frisch MJ, Trucks GW, Schlegel HB, Scuseria GE, Robb MA, Cheeseman JR, et al. Gaussian 03, Revision B.01. Pittsburgh: Gaussian, Inc.; 2003.
[68] Conciatori AB, Trapasso LE, Stackman RW. In: Mark HF, editor. Encyclopedia of polymer science and technology, vol. 14. New York: John Wiley & Sons; 1971. p. 580.
[69] Furukawa T, Date M, Nakajima K, Kosaka T, Seo I. Jpn J Appl Phys 1986;25:1178–82.
[70] Solymar L, Walsh D. Lectures on the electric properties of materials. 4th ed. Oxford: Oxford University Press; 1988.
[71] Scott AP, Radom L. J Phys Chem 1996;100:16502–13.
[72] Davis GT, Furukawa T, Lovinger AJ, Broadhurst MG. Macromolecules 1982;15:329–33.
[73] Lovinger AJ, Furukawa T, Davis GT, Broadhurst MG. Polymer 1983;24:1225–32.
[74] Lovinger AJ, Furukawa T, Davis GT, Broadhurst MG. Polymer 1983;24:1233–9.
[75] Tashiro K, Takano K, Kobayashi M, Chatani Y, Tadokoro H. Polymer 1984;25:195–208.
[76] Bellet-Amalric E, Legrand JF. Eur Phys J B 1998;3:225–36.
[77] Clark ES, Muus LT. Z Kristallogr 1962;117:119–27.
[78] Clark ES, Muus LT. Z Kristallogr 1962;117:108–18.
[79] Weeks JJ, Clark ES, Eby RK. Polymer 1981;22:1480–6.
[80] Rae PJ, Brown EN. Polymer 2005;46:8128–40.
[81] Beall GW, Murugesan S, Galloway HC, Koeck DC, Jarl J, Abrego F. Polymer 2005;46:11889–95.